



## Untargeted metabolomics as a tool to monitor biocontrol product residues' fate on field-treated *Prunus persica*



Mélina Ramos<sup>a,b,c,\*</sup>, Hikmat Ghosson<sup>a</sup>, Delphine Raviglione<sup>a</sup>, Cédric Bertrand<sup>a,d</sup>, Marie-Virginie Salvia<sup>a</sup>

<sup>a</sup> PSL Université Paris: EPHE-UPVD-CNRS, USR 3278 CRIOBE, Université de Perpignan, 52 Avenue Paul Alduy, 66860 Perpignan Cedex, France

<sup>b</sup> Institute of Food and Agricultural Technology-CIDSAV-XaRTA, University of Girona, Campus Montilivi, 17003 Girona, Spain

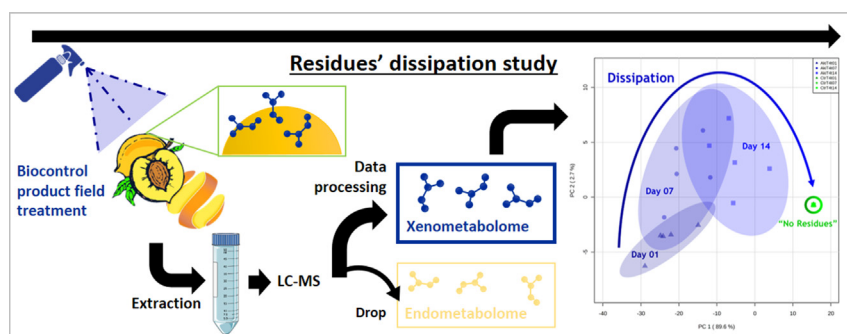
<sup>c</sup> Laboratori Fisiologia Vegetal, Facultat de Ciències, Universitat Autònoma de Barcelona, E-08193 Bellaterra, Spain

<sup>d</sup> S.A.S. AkinaO, Université de Perpignan, 52 Avenue Paul Alduy, 66860 Perpignan Cedex, France

### HIGHLIGHTS

- Innovative untargeted metabolomics approach to study PPPs residue on fruits.
- 3 PPPs' residues were monitored on *Prunus persica* in field conditions.
- "Dissipation interval" for the 3 products were investigated.
- Kinetic patterns of product compounds and degradation by-products were highlighted.
- The approach was proven reliable. Nonetheless, field experiments must be improved.

### GRAPHICAL ABSTRACT



### ARTICLE INFO

#### Article history:

Received 23 July 2021

Received in revised form 16 September 2021

Accepted 27 September 2021

Available online 2 October 2021

Editor: Yolanda Picó

#### Keywords:

Biocontrol products  
Residues monitoring  
Pesticide dissipation  
Metabolomics  
Liquid Chromatography-Mass Spectrometry

### ABSTRACT

Evidence of chemical plant protection products' (PPPs) long-term impact has been found in all environmental compartments. Therefore, other types of PPPs are developed to complement chemical PPPs like PPPs from natural sources, namely biocontrol products (BPs). Little is known about those new BPs, and it is important to assess their potential long-term environmental impact. Recently, the Environmental Metabolic Footprinting (EMF) approach was developed. It permits studying sample's entire meta-metabolome (endometabolome and xenometabolome) through a kinetics tracking of metabolomes of treated and untreated samples. Those metabolomes are compared time-by-time to estimate the "resilience time" of the samples after treatment. The current study aims to investigate BP residues' dissipation on peach fruits (*Prunus persica*). For that, an untargeted Liquid Chromatography-Mass Spectrometry metabolomics approach based on the EMF was optimised to separate the xenometabolome of the PPP from the endometabolome of the fruits. This "new version" of the EMF approach is able to target the BP treatment residues' (xenometabolome) dissipation exclusively. Thus, it is able to determine the time needed to have no more residues in the studied matrix: the "dissipation interval". Field experiment was conducted on peach tree orchard against brown rot treated with (i) a plant extract BP (Akivi); (ii) a reference mineral extract BP (Armcarb®); and (iii) a Chemical reference treatment campaign. Formulated Akivi and its by-products dissipation was monitored, a degradation kinetics appeared but the sampling did not last long enough to allow the determination of the "dissipation interval". Armcarb® and the Chemical reference's residues and by-products showed a persistence pattern along the sampling kinetics. These results indicate that the EMF approach, formerly developed on soil and sediment, is applicable for fruit matrices and can be used to investigate the fate of complex BP treatment on the matrix through the xenometabolome tracking on treated fruits.

© 2021 The Authors. Published by Elsevier B.V. This is an open access article under the CC BY-NC-ND license (<http://creativecommons.org/licenses/by-nc-nd/4.0/>).

\* Corresponding author at: PSL Université Paris: EPHE-UPVD-CNRS, USR 3278 CRIOBE, Université de Perpignan, 52 Avenue Paul Alduy, 66860 Perpignan Cedex, France.  
E-mail addresses: [melina.ramos@univ-perp.fr](mailto:melina.ramos@univ-perp.fr), [melina.ramos66@gmail.com](mailto:melina.ramos66@gmail.com) (M. Ramos).

## 1. Introduction

Plant protection products (PPPs) are products used in agriculture to prevent, to destroy, or to control any pest or disease that harm or interfere with the agricultural production (FAO, 2006). Chemical PPPs present various issues in terms of environmental and health impact. Therefore, other types of PPPs are developed to complement chemical PPPs, e.g. biocontrol products (BPs) that are increasingly being promoted by several governments (European Parliament and Council Of The European Union, 2009; Ministère de l'Agriculture et de l'Alimentation, 2015). BPs are PPPs from natural sources, i.e. molecules or organisms that already exist as it is within nature, like botanical extracts or beneficial bacteria. The development of these new BPs requires the development of new methodologies in order to monitor their residues' dissipation, which is a compulsory step to put any PPP on the market.

At present, the existing methodologies are only adapted for chemical PPPs. For instance, some of them are described by the Organisation for Economic Co-operation and Development (OECD) in the international guidelines for the testing of chemicals (OECD, 2007a), currently used by several institutions delivering marketing authorisations (e.g.: the French agency "Agence Nationale de Sécurité Sanitaire de l'Alimentation, de l'Environnement et du Travail (ANSES)"; the Spanish agency "Instituto Nacional de Investigación y Tecnología Agraria y Alimentaria (INIA)"; the European Union agency "European Food Safety Authority (EFSA)"). The section describing methodologies to monitor PPPs residues' metabolism in crops (OECD, 2007b) will be explained as follows: The component of a PPP that works against the pathogen is called Active Substance (AS). For approval processes, that AS must be well characterised in terms of structure, chemical-physical properties, and mode of action. Moreover, PPP residue monitoring in treated plants can be conducted through isotopic labelling of the AS (OECD, 2007b). The different moieties of the molecule are radiolabelled using  $^{14}\text{C}$ ,  $^{32}\text{P}$ , or  $^{35}\text{S}$  radioisotopes so that all significant parts can be tracked. Crop grown in laboratory-controlled conditions are treated with radiolabelled AS and its behaviour within the plant is studied. Radioactive labelled molecules are extracted and 90% of the Total Radioactive Residues (TRR) must be identified representing the AS and its major by-products (OECD, 2007b). Degradation of PPP are determined by various processes that can be classified in 2 types: (1) biotic degradation and (2) abiotic degradation, among which hydrolysis (acid, alkaline, or enzymatic), oxidation, reduction, or photolysis. The domination of a degradation pathway depends on various parameters like the chemical-physical properties of the molecule, the weather (e.g. light, pH), or the type of application used for the treatment. For example, aerial plant parts treatments are more subject to photodegradation. Once identified, the dissipation of the AS and its major by-products is measured within the crop and in soils. The dissipation times of 50% of the AS's initial amount "DT50" and of 90% of the AS's initial amount "DT90" are studied particularly (European Commission – Directorate General for Agriculture, 2000). Their values, expressed in days, may lead to further investigations. For example, if the DT90 in soils is higher than 100 days, complementary study on next rotation culture is necessary (European Commission – Directorate General for Agriculture, 2000).

However, guidelines reporting monitoring methods for BPs are neither available for crops, nor for soils and sediments. The previously described methodologies for chemical PPPs are not suitable for BPs as the ASs of BPs are very rich and complex mixtures, with a relatively large number of unidentified components. There are 3 types of BPs affected by marketing authorisation processes (ITAB and ONEMA, 2013): (1) living or part of microorganisms: fungi, bacteria or virus; (2) extracts from natural sources: mineral, botanical or animal sources; and (3) semiochemicals: pheromones and kairomones. In addition, BPs activities are often the result of an interaction between several of its components. Moreover, the components responsible for the main activity of the

product are usually unknown and the most abundant components are not always the most active against the pathogen. Thus, it is impossible to radiolabel such complex ASs and to determine their DT50 or DT90.

Hence, as classic residues monitoring methodologies are neither fitting to BPs, nor in crops, nor in soils or sediments, and as all or part of the components of the ASs are not identified, an untargeted approach seems to be a potential solution. Therefore, an innovative approach relying on untargeted metabolic profiling was recently developed; the Environmental Metabolic Footprinting (EMF) (Patil et al., 2016; Salvia et al., 2018). EMF concept relies on the meta-metabolome study of a treated environmental matrix versus an untreated environmental matrix along a kinetics study. This approach aims to monitor the evolution of the differences between the metabolic profiles of the treated and the untreated control matrices through time. The meta-metabolome represents the combination of the endometabolome from the original matrix and the xenometabolome from the treatment, i.e. the PPP residues composed of the ASs and the formulation ingredients of the product and their transformation by-products. On one hand, the EMF gives rise to a new integrative proxy: the "resilience time" (Patil et al., 2016; Salvia et al., 2018). It corresponds to the time needed for the xenometabolome (PPP residues) to dissipate, and for the PPP's impact on the matrix to disappear (i.e. the endometabolome of the treated samples to re-establish the same profile as that of the endometabolome of the untreated control samples at a given time point). On the other hand, the EMF is potentially useful for determining the "dissipation interval" that corresponds to the time needed to have no difference between the residues profiles of the treated sample and the profile of the control samples that must not contain residues. This investigation can be done by selecting and monitoring the xenometabolome exclusively.

The aim of the work described in this article is (i) to optimise the existing EMF approach in order to target, exclusively, the treatment residues (xenometabolome) on the fruit matrix, and (ii) to investigate BP residues' dissipation on the treated fruit matrix. In the current work, the peach carposphere was selected as a typical matrix to be studied in such a context. For that, the EMF approach formerly developed on soil (Patil et al., 2016) and sediment (Salvia et al., 2018) laboratory microcosm experiments will be adapted in the current work to peach peels from a field experiment. This study will focus on the xenometabolome selection part of the EMF, which is a challenging part. In fact, the xenometabolome isolation from the meta-metabolome must be optimised. The experiments were conducted in field conditions with a botanical extract BP; the "Akivi" (Tamm et al., 2017). This product presents direct antifungal activity due to a high content on polyphenols and terpenes. Akivi was compared in field conditions (peach orchards) with a reference BP; "Armcarb®" based on the potassium hydrogen carbonate mineral compound, and a chemical reference treatment campaign; based on a mix of 5 synthetic organic compounds (Boscalid, Fenbuconazole, Fluopyram, Pyraclostrobin and Tebuconazole). The 3 treatments modalities were used against brown rot (*Monilia fructigena*) with interesting efficacy results during this field experiment. This fungus is one of the main diseases affecting peach fruits and the agricultural sector needs new products to protect the crops due to the lack of solutions in organic farming against this disease.

## 2. Material and methods

### 2.1. Experimental design

#### 2.1.1. Field experiments

Field experiments were conducted in collaboration with the "Centre Expérimental des Fruits et Légumes du Roussillon" (Sica CENTREX). They were performed in their agricultural domain in Torrelles (France) [GPS: (DMS) 42°45'14.221"N 2°58'35.712"E] on peach trees orchard *Prunus persica* 'CORINDON®' treated against brown rot (*Monilia fructigena*). Brown rot is a post-harvest disease affecting the fruit. Thus, peaches are the main target of the treatment, so peach peel

matrix was selected for this study. Different groups of trees were treated separately with 3 products. A first group called “Aki” was treated with 0.75 kg/ha “Akivi” formulated plant extract BP (S.A.S. AkiNaO). A second group called “Arm” was treated with 5 kg/ha “Armicarb®” formulated mineral extract BP (De Sangosse) with Potassium Hydrogen Carbonate as AS. A third group called “Chi” was treated with a Chemical reference treatment campaign usually used against brown rot: first treatment with 0.75 g/ha “Signum®” (AS: Boscalid and Pyraclostrobin, BASF), second treatment with 3 L/ha “Krugatm” (AS: Fenbuconazole, Dow AgroSciences), and third treatment with 0.5 L/ha “Luna® Experience” (AS: Fluopyram and Tebuconazole, Bayer). The chemical structure of the AS of the Chemical reference modality are presented in Fig. S1. “Arm” and “Aki” treated trees were distributed in Fisher blocks of 3 replicates of 2 trees (6 trees in total); “Chi” treated trees and untreated controls “Ctr” trees were distributed in 3 replicates of 3 trees (9 trees in total) (Fig. S2). The treatment campaign was made in August 2018 with 4 treatments. The first and second treatments were spaced 15 days apart and then trees were treated every 7 days (Fig. 1).

### 2.1.2. Plant material & sampling method

For the metabolomics approach, peach samplings (Fig. 1) were made according to a kinetics beginning after the last BPs treatment (T4): one day after T4 (T4t01); 7 days after T4 (T4t07), corresponding to the harvest; and 14 days after T4 (T4t14). These kinetics points correspond to 7 days after T3 (T3t07), 14 days after T3 (T3t14) and 21 days after T3 (T3t21) respectively. T3 corresponding to the last “Chemical” treatment. Peaches were sampled in the area at the middle of the trees identified by the trees’ trunks, in order to avoid the part of the branches that can be contaminated by the next treatment. Peaches were sampled at different positions on the tree: two peaches were sampled on each side of the rank and one peach inside the foliage (Fig. S3). For each modality of time and treatment, 5 peaches were sampled in each of the 3 replicate blocks. The 15 peaches were randomly mixed and separated in 5 biological replicates of 3 fruits. The peaches were then peeled, and peels of each of the samples were stored separately in freezer-safe bags at  $-32\text{ }^{\circ}\text{C}$  until the analyses (the extractions and analyses were done at once after the end of the kinetic experiment, *i.e.* after the collection and storage of all the samples).

## 2.2. Chemical analysis

### 2.2.1. Chemicals

For sample preparation, Acetonitrile HPLC grade and Methanol HPLC grade were purchased from VWR (Fontenay-sous-Bois, France). For UHPLC-HRMS analysis, water LC-MS grade was purchased from VWR (Fontenay-sous-Bois, France), and Methanol LC-MS grade was purchased from Carlo Erba (Val de Reuil, France). Formic acid 99% (for analysis) was obtained from Acros Organics (Geel, Belgium). Boscalid, Diclofenac, Fenbuconazole, Fluopyram, Progesterone, Pyraclostrobin, and Tebuconazole analytical standards were obtained from Sigma-Aldrich (Saint Quentin-Fallavier, France).

### 2.2.2. Sample preparation

Before extraction, samples were put in the freezer ( $-32\text{ }^{\circ}\text{C}$ ) overnight prior to freeze-drying (Heto, FD3) that lasted 48 h. The peach peel content of each freezer-safe bag, corresponding to one laboratory repetition, was then grinded. 4.50 g ( $\pm 0.05\text{ g}$ ) of the dry peach peel powder were transferred into a 50 mL tubes (Fisher Scientific) in order to perform the extraction with 40 mL of acetonitrile. Acetonitrile was chosen as a classic extraction solvent used for PPPs residues’ studies (Rajski et al., 2014; Rizzetti et al., 2016; Rutkowska et al., 2018). A one-step-based extraction protocol was set in order to reduce sample manipulation-linked biases and uncertainties. The protocol was as follows: all the tubes were manually shaken, swirled for 1 min on Vortex shaker (Heidolph, Hei-MIX Multi Reax), and then put on an agitation table (Benchmark Scientific, BV1010) for 20 min at 500 RPM. After, a centrifugation is performed for 10 min at 4500 RPM and room temperature ( $\sim 20\text{ }^{\circ}\text{C}$ ). Then, the supernatant was transferred into vials after filtration through  $0.22\text{ }\mu\text{m}$  PTFE filters. The final extract is diluted by a dilution factor of 2 in methanol. An internal standard composed of a mix of Diclofenac and Progesterone is added to the sample at a concentration of 5  $\mu\text{g/mL}$  for each of the two molecules.

### 2.2.3. UHPLC-HRMS analysis

Metabolic profiling analyses of the extracts of peach peels were achieved by Ultra High Performance Liquid Chromatography-High Resolution Mass Spectrometry (UHPLC-HRMS) using a Vanquish™ Flex UHPLC hyphenated with a QExactive™ Plus Heated Electrospray-Quadrupole/C-Trap-Orbitrap Mass Spectrometer (Thermo Fisher

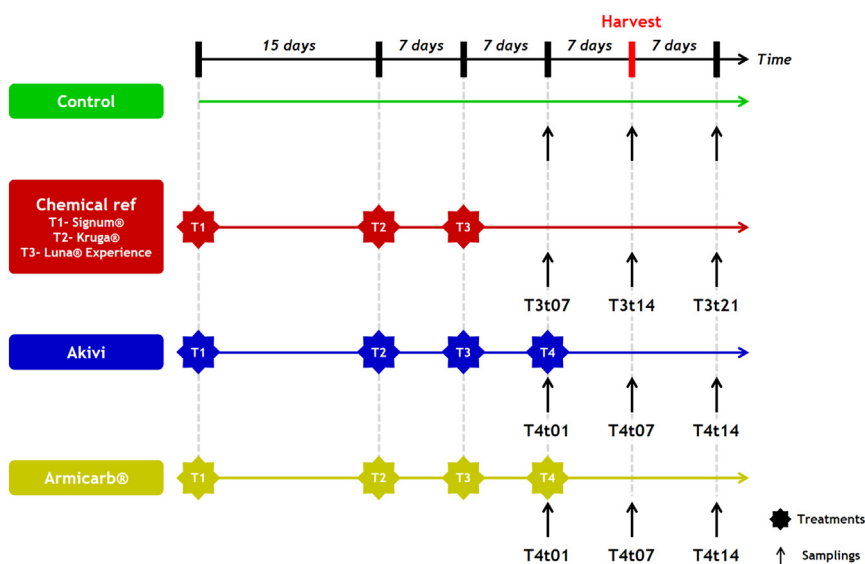


**Fig. 1.** Peach field-sampling campaign after the 4 different treatments modalities: (i) the untreated Control (green); (ii) first treatment (T1) with Signum®, second treatment (T2) with Kruga®, and third treatment (T3) with Luna® Experience for the Chemical reference (red); (iii) 4 treatments with a plant extract BP Akivi (blue); and (iv) 4 treatments with a mineral extract BP Armicarb® (yellow).

Scientific). Metabolites were separated on a Luna® Omega 1.6 µm Polar C18 100 Å, 100 × 2.1 mm column (Phenomenex) put in an oven set at 30 °C. 5 µL of extract were injected. A gradient-based separation was applied with the following mobile phases: water/methanol 65:35 v/v + 0.1% formic acid (v/v) (A), and methanol +0.1% formic acid (v/v) (B). The mobile phase flow was maintained at 0.35 mL/min. The gradient program was the following: initially 2 min with 0% (B), then from 0% to 70% (B) in 3 min, from 70% to 100% (B) in 11 min, 6 min at 100% (B), and from 100% to 0% (B) in 1 min back to initial conditions that were maintained for 2 min with 0% (B). Each run lasted for 25 min in total. For the HRMS conditions, the acquired RT range was between 2 and 23 min (in Full MS). The Heated Electrospray (HESI) was operated in positive mode (ESI+). Sheath gas (N<sub>2</sub>) flow rate was set to 35 arbitrary units (a.u.); auxiliary gas (N<sub>2</sub>) flow rate was set to 10 a.u.; sweep gas (N<sub>2</sub>) flow rate was equal to 0 a.u.; capillary temperature was equal to 320 °C; auxiliary gas temperature was 200 °C; spray voltage was set to 3.2 kV; and the S-lens RF level was 50.0. The mass spectra were acquired in a scanning range of 200–1500 *m/z* in “Profile” acquisition mode. The resolution was set to 35,000 at a *m/z* equal to 200; the Automatic Gain Control Target of the C-Trap was set to 3e6 charges, the Maximum Injection Time to the Orbitrap was equal to 200 ms. Samples of all time points and treatment modalities were prepared and analysed at once in a random order. Blank extraction samples were injected at the beginning of each of the two analytical batches. The blank extraction samples correspond to acetonitrile that underwent all extraction steps without peach peel sample addition. Three different Quality Control (QC) pool samples – each is specific to one treated group (“Aki”, “Arm”, “Chi”) – were injected every 8 samples in order to assess the analytical variations during data acquisition. Each QC pertaining to a treatment group was prepared by mixing an equal volume from 3 out of 5 treated samples of the group for each time point.

#### 2.2.4. Quantification of chemical reference ASs

The 5 chemical product ASs (Boscalid, Pyraclostrobin, Fenbuconazole, Fluopyram and Tebuconazole) were quantified in some peach peel samples using the standard addition method. The quantification was carried out within 3/5 repetitions of both contaminated control “Ctr” samples and treated “Chi” samples at the last sampling point: 21 days after the third treatment. The ranges of spiking concentrations, that comprised 4 points, were different for the “Ctr” and “Chi” samples. For the “Ctr” samples, the calibration curve was made from 0 (no addition) to 20 ng/mL. For the “Chi” samples, the calibration curve was made from 0 to 200 ng/mL.

#### 2.3. Software and data processing

LC piloting, LC-MS hyphenation, analytical sequence piloting and UHPLC-HRMS data acquisitions were performed using Xcalibur 4.1.31.9 (Thermo Fisher Scientific). The Mass Spectrometer and the HESI source were configured using Q Exactive Plus – Orbitrap MS 2.9 build 2926 software (Thermo Fisher Scientific). Data were acquired in RAW format. They were then converted to “.mzML” using the MSConvertGUI software (ProteoWizard) (Chambers et al., 2012) in order to upload and process them using Galaxy Workflow4Metabolomics platform (Giacomini et al., 2015; Guitton et al., 2017). Data of the three different PPP treatments modalities were processed using the same workflow but separately (i.e. “Aki” vs. “Ctr”; “Arm” vs. “Ctr”; “Chi” vs. “Ctr”). The pre-processing workflow and all its parameters are published on the Galaxy Workflow4Metabolomics platform (Ramos, 2021). The “XCMS” algorithm-based pre-processing (Smith et al., 2006) consisted of a “centWave” peak picking (Tautenhahn et al., 2008), “PeakDensity” peak grouping, loess/non-linear “PeakGroups” retention time adjustment (degree of smoothing: 0.8), peak filling and “CAMERA” peak annotation (Kuhl et al., 2012). For the retention time adjustment, the “PeakGroups” algorithm used the chromatographic peaks corresponding to the internal standards (among others). Indeed, these reference peaks are present in all

samples, pools and blank extractions and are used in order to correct the retention times of the chromatographic peaks of the compounds. The considered signal value for ion features was the chromatographic peak area. The first three “raw” matrices obtained for each of the three treatments contained an important number of features (16058 for “Aki”, 11717 for “Arm”, and 11310 for “Chi”). Such large numbers of variables render difficult the data handling and the statistical analyses. Hence, matrices clean-up should be performed. Therefore, a first clean-up was performed in order to eliminate all features that are significantly detected in blanks (based on p-Values and t-Stat outputs generated by the “CAMERA” step). Then, as analytical drifts could occur in LC-MS sequences, an “inter/intra-batch” signal correction was applied using the “Batch correction” function with a “loess” regression model (span = 0.8) (van der Kloet et al., 2009). “Loess” regression model was chosen because it better fits the variation of the peak intensities over the analytical sequence than a “linear” regression model (span = 0). A span lower than 1 was selected (span = 0.8) in order to avoid the overestimation of the outliers. This step was followed by a second clean-up according to feature’s CV in pool QC injections (all features with area RSD upper than 30% through pool QC injections were eliminated from the dataset) (Thévenot et al., 2015). A third clean-up was then applied in order to eliminate ion redundancies as much as possible (the ion with the highest intensity was selected as the representative ion). This elimination was done using the Analytic Correlation Filtration approach developed by Monnerie et al. (2019). After generating those “intermediate” data matrices, significant features were filtered in order to select xenometabolites exclusively, as the current work is focused on BPs residues. This filtration was performed following two main steps: 1) features showing significant intensity folds between the treated and the untreated samples were selected (p-Value ≤ 0.05 and Fold Change ≥ 5 with a higher intensity in the treated samples), and 2) features detected in the untreated control samples were eliminated after a manual investigation of their EICs was carried out using Xcalibur 4.1.31.9. After the mentioned pre-processing, clean-ups and filtration were achieved, three different “final” matrices pertaining to the three investigated products were obtained, with 382 features for the “Aki” xenometabolome data matrix, 14 features for the “Arm” xenometabolome data matrix, and 17 features for the “Chi” xenometabolome data matrix. Statistical analyses were then performed on those final matrices.

#### 2.4. Statistical analysis

Statistical analysis was made using the R-based MetaboAnalyst platform (Pang et al., 2021). Pareto scaling was conducted to normalise the data prior to make Principal Component Analysis (PCA), Orthogonal Projections to Latent Structures-Discriminant Analysis (OPLS-DA), and boxplots of the features. For the Heatmaps, data scaling and normalisation were not suitable, as this type of analysis was conducted in order to visualise the dissipation of molecular traces in samples through the time. Thus, only a Log<sub>10</sub> transformation was applied before this analysis in order to minimise the “size effect” of the peaks with high intensity (that can hide the other peaks with low but non-null intensity). The  $-\infty$  values (issued from the Log<sub>10</sub> transformation of intensities originally equal to 0) were converted to 0 in order to adjust the intensity scale and to allow null intensities to be observable.

##### 2.4.1. Principal component analysis

PCA is a descriptive unsupervised multivariate statistical model. It relies on linear combinations of the correlating variations associated to variables in the dataset. The PCA aims to simplify the variations by combining them and then to identify the combinations giving the best explanation of the systematic variations in the dataset. Those combinations are the principal components (PCs); they are associated with a value in per cent representing the ability of each PC to explain a variation in the dataset. Usually, the PCs with the highest percentages of variance explanation are selected to project the samples in a 2D-



graph. Then, the samples are projected on the graph and can be grouped or clustered according to the degree of similarity of their variables profiles, *i.e.*, their metabolic profiles when it comes to metabolomics.

#### 2.4.2. Orthogonal projections to latent structures discriminant analysis

OPLS-DA is an explicative supervised multivariate statistical model (Trygg and Wold, 2002). It relies on the linear combinations of the correlating variations associated to variables like in the PCA, but it identifies the combinations giving the best explanation of the data variance correlating to a defined experimental factor. Moreover, it separates the predictive variation (horizontal axis) representing the variation that is correlated with the defined factor (*i.e.* the predictive component “p”), from the orthogonal variations (vertical axis) representing some systematic variations that are uncorrelated (orthogonal) to the defined factor (*i.e.* the orthogonal components “o<sub>(n)</sub>”). This multivariate analysis is a model that needs to be validated. Therefore, a Cross-Validation (CV) test should be performed. It provides different scores for each of the components that are needed for the assessment of the model: The R2X representing the percentage of the variation explained by the component; the R2Y representing the correlation coefficient of the samples' discrimination to the component; and the Q2 representing the predictivity of the component. For the “p” component, the model performance is given by the R2Y<sub>(p)</sub> value that has to be close to 1; the model predictivity is given by the Q2<sub>(p)</sub> value that has to be >0.5 in metabolomics studies; the R2Y<sub>(p)</sub> should be higher than the Q2<sub>(p)</sub>; and R2Y<sub>(p)</sub> – Q2<sub>(p)</sub> should be lower than 0.3 (Wiklund, 2008). For the “o” component, the R2Y<sub>(o)</sub> and Q2<sub>(o)</sub> values should be as low as possible; if the values are >0.5 it compromises the validation of the model (Wiklund, 2008).

To ensure that the difference explained by the OPLS-DA model is the result of a real effect caused by the defined factor, and not due to a random effect, a permutation test must be performed. The “original” model represents the model that has been constructed after sorting samples according to the defined factor. The samples are then mixed up by the permutation test in new random groups for several times (the test randomly permutes samples in between the different groups). For each random distribution, an OPLS-DA model is then constructed and for each model, as well as for the “original” model, a CV test is performed. After, the permutation test calculates a p-Value defined as:

$$p\text{-Value} = \frac{(\text{number of permutations giving better model than the "original" model})}{(\text{total number of permutations})}$$

The total number of permutations is set here to 1000. p-Values lower than 0.05 must be obtained, *i.e.* there is less than 5% of chance that the mixed model is better than the “original” one. Thus, there is less than 5% of probability that the discrimination between samples is due to a random effect instead of being caused by an effect related to the defined factor.

#### 2.4.3. Heatmaps

A Heatmap is a 3D visualisation technique combining a vertical axis, a horizontal axis and a colour scale within the map. The vertical axis represents the features classified by similarities between each other thanks to a Dendrogram-based hierarchical clustering (Distance Measure: Euclidean; Clustering Algorithm: Ward). The horizontal axis represents the samples classified by treatment modality and by kinetics sampling points. The colour scale represents the intensity of the features from 0 in dark blue to the most intense in dark red.

### 3. Results

After generating the “final” data matrices, xenometabolome of each studied product vs. the untreated control are analysed separately (in separated datasets): 1) Akivi; the botanical extract BP, 2) Armicarb®;

the mineral extract BP used as BP reference on the field experiment, and 3) the Chemical reference composed of 3 treatments with 5 chlorinated compounds (Fig. S1). Due to the exclusive selection and filtering of the xenometabolome in the data matrices, untreated control samples are all at a total relative intensity level equal to 0 (except for the data matrix of the Chemical reference; the reason will be explained subsequently). The untreated control samples profiles thus represent the “No Residues” point that must be reached in order to determine the “dissipation interval”.

#### 3.1. Akivi

Akivi final xenometabolome data matrix is visualised on a Heatmap after a Log<sub>10</sub>-transformation and a conversion of  $-\infty$  values to 0 were applied (Fig. 2). 382 xenometabolite features are detected. The Akivi treated samples “Aki” are put in column on the left side (in blue) and the “Ctr” untreated control samples are put on the right side (in green). Within the 2 modalities, the samples are arranged by time sampling from the left (T4t01) to the right (T4t14). On the ordinate axis, the features are represented and sorted following the Euclidean Distances through samples. Inside the Heatmap, the features are coloured according to their relative intensity from 0 in dark blue to the highest intensity in dark red (on a Log<sub>10</sub> scale).

A global dissipation pattern for the Akivi treated samples along time is observed. In fact, relative intensities of features seem to be decreasing from T4t01 to T4t14, and some of the features have completely disappeared 14 days after T4 (T4t14). However, the “No Residues” point is not reached. In order to investigate closely the features behaviour, boxplots of the features along the time samplings are observed and their behaviour can be grouped into 4 blocks from A to D, respectively from the less persistent to the most persistent features. In fact, boxplots representing block A pattern (Fig. S4A) show a quick dissipation kinetics with total disappearance 14 days after T4 (T4t14). Boxplots representing block B pattern (Fig. S4B) show a certain persistence between T4t01 and T4t07 but quick dissipation between T4t07 and T4t14 and nearly reaching disappearance 14 days after T4 (T4t14). On the contrary, boxplots representing block C pattern (Fig. S4C) show quick dissipation between T4t01 and T4t07 but persistence at low intensity level between T4t07 and T4t14. Eventually, boxplots representing block D pattern (Fig. S4D) show persistence at high intensity between T4t01 and T4t07 but certain dissipation between T4t07 and T4t14 with persistence at low intensity 14 days after T4 (T4t14). Therefore, the Heatmap visualisation is able to show a global dissipation of the features that must represent the molecules belonging to the “Aki” extract within the treated samples. However, this model is not able to underline any by-product appearance patterns. Thus, PCA is used in order to search for such patterns, by projecting the “Aki” xenometabolome data matrix after Log<sub>10</sub>-transformation and Pareto scaling were applied (Fig. 3).

The samples are projected on the 2 most relevant principal components: PC1 and PC2. The PC1 explains 89.6% of the variations. It discriminates the Akivi treated samples “Aki” (in blue) from the “Ctr” untreated control samples (in green –all grouped in one point representing the “No Residues” point (the “0” point)–). PC1 also discriminates the “Aki” treated samples T4t01 from the group T4t14 that heads to the “No Residues” point. On the other hand, the PC2 explaining 2.7% of the variations discriminates the “Aki” treated samples T4t01 from the groups T4t07 and T4t14. All these observations could be explained by the disappearance of features from the original BP applied on the peach peels –characteristic of the T4t01 group–, and with the appearance of by-products features at T4t07 and their disappearance within T4t07 and T4t14. To verify this hypothesis, the loading plots of the PCA are observed (Fig. S5). The features at the bottom of the loadings plot are most intense within the “Aki” treated samples at T4t01. The boxplots of these features represented in Fig. S6A show a quick dissipation patterns with total dissipation 14 days after T4 (T4t14). Whereas, the features at the top of the loadings plot (Fig. S3) present the highest

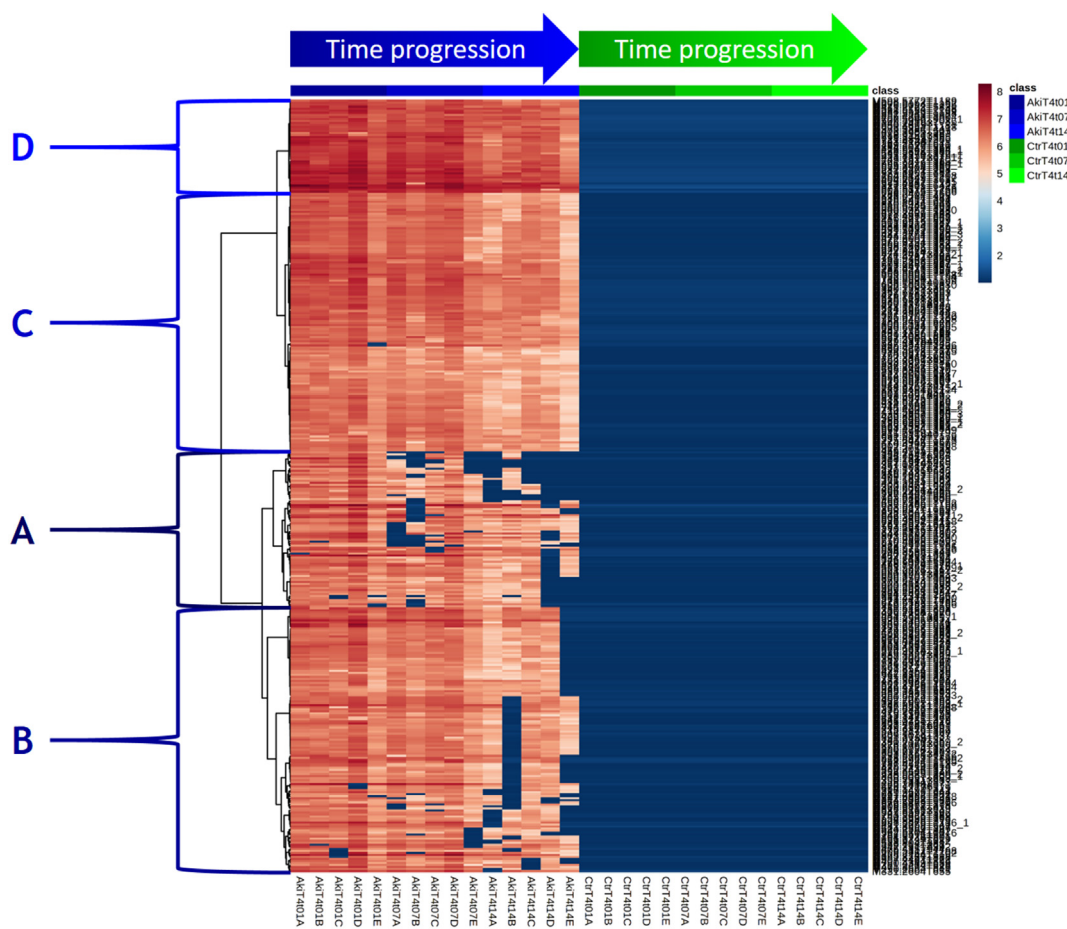


**Fig. 2.** Heatmap of Akivi xenometabolites abundance (the darker is the red, the higher is the intensity). “Aki” treated samples from 1 day (dark blue) to 14 days (light blue) after treatment, vs. “Ctr” untreated control samples from 1 day (dark green) to 14 days (light green) after treatment. (A, B, C, D): Blocks of features’ dissipation patterns from the less persistent (A) to the most persistent (D).

intensities within the “Aki” treated samples at T4t07. The boxplots of these features represented in Fig. S6B show by-product evolution patterns. That is to say, a higher intensity at T4t07 than at T4t01 and a dissipation between T4t07 and T4t14. On another hand, the “Aki” treated samples vs. the “Ctr” untreated control samples from the Akivi xenometabolome data matrix are compared for each sampling time point using the OPLS-DA after a  $\text{Log}_{10}$ -transformation and a Pareto scaling were applied (Table S1). The OPLS-DA model is validated for every time sampling ( $R2Y > R2X$ ,  $R2Y > Q2$ ,  $R2Y - Q2 \leq 30\%$ , and  $Q2 > 50\%$  (Wiklund, 2008)) but the values decrease from 1 day after T4 ( $R2Y$ : 97.20%,  $Q2$ : 96.70%) to 14 days after T4 ( $R2Y$ : 89.90%,  $Q2$ : 87.80%). These results support the interpretation claiming that the Akivi xenometabolome is dissipating as discussed above.

### 3.2. Armicarb®

Armicarb® is a mineral extract and its AS is Potassium Hydrogen Carbonate salt ( $\text{KHCO}_3$ ). This compound has a high solubility in water, which renders difficult its retention on the C18 column. Thus, the analytical method is not able to detect the AS but it should be able to detect some of the co-formulants and adjuvants. In fact, 14 xenometabolites features are detected. Armicarb’s® final xenometabolome data matrix is visualised on a Heatmap after a  $\text{Log}_{10}$ -transformation and a conversion of  $-\infty$  values to 0 were applied (Fig. 4). The Armicarb® treated samples “Arm” are put in column on the left side (in yellow) and the “Ctr” untreated control samples are put on the right side (in green). Within the 2 modalities, the samples are arranged by time sampling from the left (T4t01) to the right

(T4t14). On the ordinate axis, the features are represented and sorted following the Euclidean Distances through samples. Inside the Heatmap, the features are coloured according to their relative intensity from 0 in dark blue to the highest intensity in dark red (on a  $\text{Log}_{10}$  scale).

No specific patterns can be observed. Heatmap visualisation of “Arm” xenometabolome data matrix shows persistence of the detected xenometabolites of the product. To investigate these data further, PCA is used to analyse “Arm” xenometabolome data matrix after a  $\text{Log}_{10}$ -transformation and a Pareto scaling were applied (Fig. 5). The samples are projected on the 2 most relevant principal components: PC1 and PC2. PC1, explaining 82.7% of the variations, is discriminating the Armicarb® treated samples “Arm” in yellow from the “Ctr” untreated control samples in green all grouped in the “No Residues” point.

The PCA is not able to discriminate the Armicarb® treated samples by time sampling even if it shows a tendency of the day 14 after T4 (T4t14) samples to head to the “No Residues” point compared with the other samples. In fact, boxplots of one of those features are shown in (Fig. S7). They show a degradation tendency pattern and an almost disappearance 14 days after T4. Moreover, the Armicarb® treated samples vs. the untreated control samples are compared for each time sampling using OPLS-DA after a  $\text{Log}_{10}$ -transformation and a Pareto scaling were applied to the Armicarb® xenometabolome data matrix (Table S2). The OPLS-DA model is validated for every time sampling ( $R2Y > R2X$ ,  $R2Y > Q2$ ,  $R2Y - Q2 \leq 30\%$ , and  $Q2 > 50\%$  (Wiklund, 2008)) but the values decrease from 1 day after T4 ( $R2Y$ : 97.20%,  $Q2$ : 97.20%) to 14 days after T4 ( $R2Y$ : 84.20%,  $Q2$ : 79.10%). These results are concordant with the results previously observed

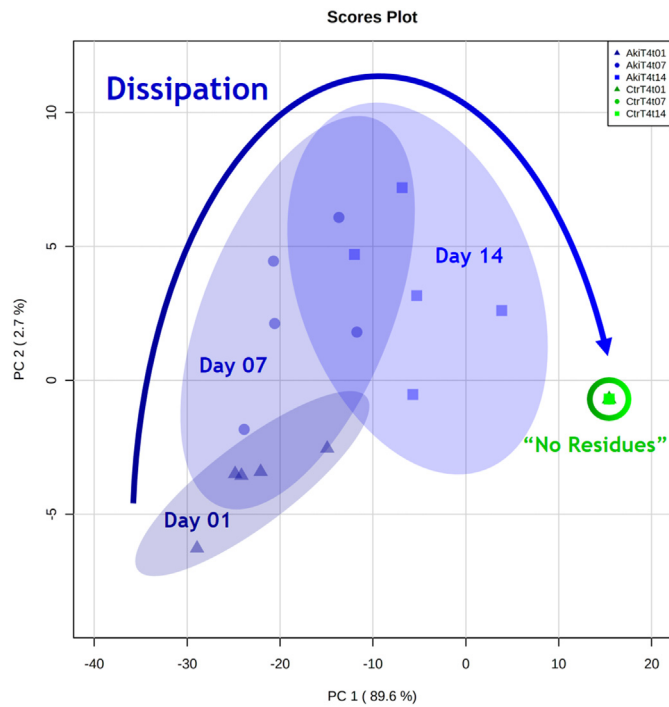


**Fig. 3.** PCA of Akivi xenometabolites degradation kinetics: 1 day after the fourth treatment (T4) (T4t01), 7 days after T4 (T4t07), 14 days after T4 (T4t14) (from dark blue to light blue, respectively), and the “No Residues” point in green, assembling all “Ctr” samples.

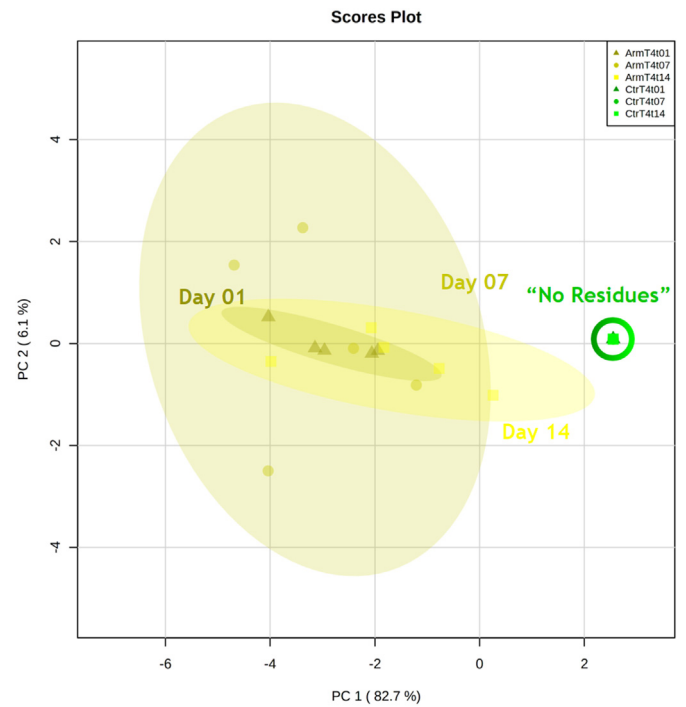


**Fig. 5.** PCA of Armicarb® xenometabolites: 1 day after the fourth treatment (T4) (T4t01), 7 days after T4 (T4t07), 14 days after T4 (T4t14) (from dark yellow to light yellow, respectively), and the “No Residues” point in green, assembling all “Ctr” samples.

with the PCA (Fig. 5) showing a global persistence of the detected Armicarb® xenometabolites with a dissipation tendency observed 14 days after T4.

### 3.3. Chemical reference

The Chemical reference treatment campaign is composed of 3 different treatments with 3 different products as described on Fig. 1.

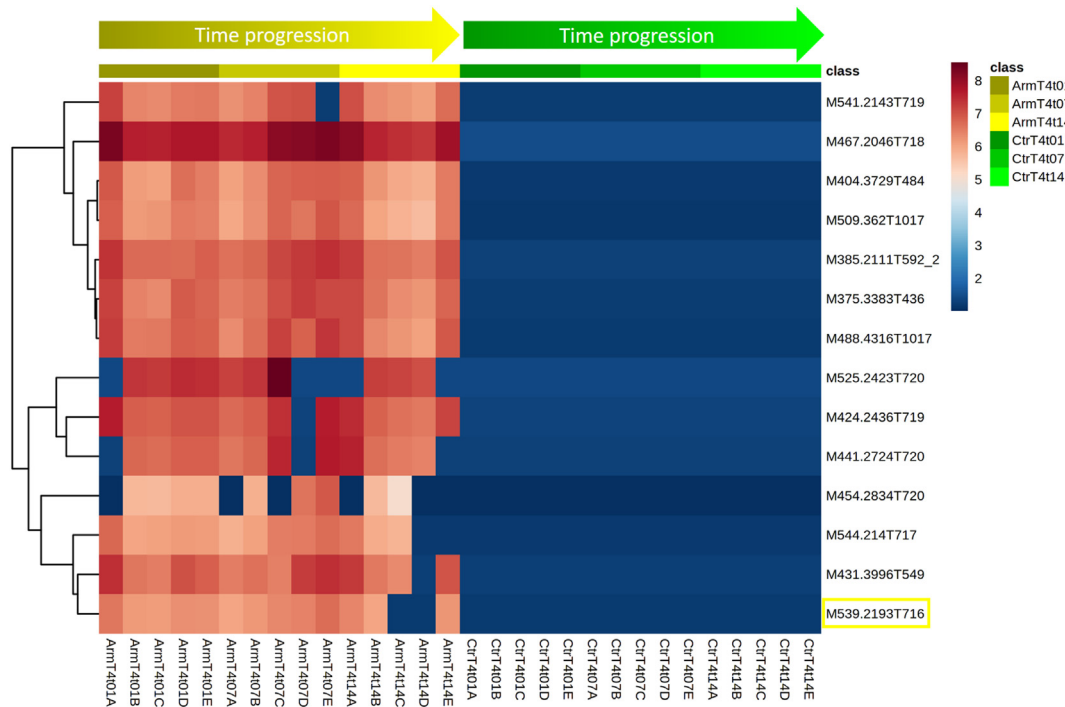


**Fig. 4.** Heatmap of Armicarb® xenometabolites abundance (the darker is the red, the higher is the intensity). “Arm” treated samples from 1 day (dark yellow) to 14 days (light yellow) after treatment, vs. “Ctr” untreated control samples from 1 day (dark green) to 14 days (light green) after treatment.

**Table 1**  
Exact masses of the active substances of the chemical reference treatment campaign.

Application order	Product	Active substance (AS)	CAS number	Exact monoisotopic mass [M] (g/mol)	[M + H] <sup>+</sup> (m/z)
1st	Signum® (BASF)	Boscalid	188425-85-6	342.0327	343.0399
		Pyraclostrobin	175013-18-0	387.0986	388.1059
2nd	Kruga® (Dow)	Fenbuconazole	114369-43-6	336.1142	337.1215
3rd	Luna® Experience (Bayer)	Tebuconazole	107534-96-3	307.1451	308.1524
		Fluopyram	658066-35-4	396.0464	397.0537

The AS of the 3 different products (5 different molecules in total) are well-known, their chemical structures are presented Fig. S1 and their exact masses are summarised in Table 1.

Considering that the ASs are all chlorinated (Fig. S1) and their exact masses are known, they were detected and identified within the xenometabolome data matrix “Chi”, except the Tebuconazole that was detected and identified within the global data matrix only (the matrix acquired before the clean-up process). As the features of those compounds were identified, their presence in the untreated control samples “Ctr” was noticed. These compounds were thus contaminating the “Ctr” samples with a relatively low rate (their intensities are 5-times higher in “Chi” than in “Ctr” (Fold Change (FC) > 5), except for the Tebuconazole (Fig. S8) –which explains its disappearance from the data matrix after filtering features with FC < 5–). In order to avoid introducing any bias during the data analysis, the subsequent investigations (statistical analyses) are pursued on the final xenometabolome data matrix “Chi” containing the 4 compounds only (Boscalid, Pyraclostrobin, Fenbuconazole and Fluopyram). Moreover, all the compounds exclusively detected within the chemically treated samples and showing Chlorine isotope Mass Spectrometry patterns with a FC > 5 were considered in the “Chi” xenometabolome data matrix. Therefore, in this part of the results, the “No Residues” point is not an overall point of untreated control samples as it considers the presence of the contaminations. It will be thus referred as “contaminated untreated control samples” (“Ctr”).

All MS spectra with Chlorine isotopic patterns belonging to the products’ xenometabolome are summarised in Fig. S9. The *m/z* peaks of the principal ions “[M + H]<sup>+</sup><sub>35</sub>Cl” and their “[M + H]<sup>+</sup><sub>37</sub>Cl” and “[M + H]<sup>+</sup><sub>37</sub>Cl<sub>2</sub>” *m/z* peaks are circled in red. Chemical final xenometabolome data matrix is visualised on a Heatmap after a Log<sub>10</sub>-

transformation and a conversion of  $-\infty$  values to 0 were applied (Fig. 6). The chemically treated samples “Chi” are put in column on the left side (in red) and the untreated control samples “Ctr” are put on the right side (in green). Within the 2 modalities, the samples are arranged by time sampling from the left (7 days after T3) to the right (21 days after T3). On the ordinate axis, the features are represented and sorted following the Euclidean Distances through samples. Inside the Heatmap, the features are coloured according to their relative intensity from 0 in dark blue to the highest intensity in dark red (on a Log<sub>10</sub> scale). Concerning the 4 identified compounds of the ASs, they are circled in red on the Heatmap and they present a persistent pattern along the kinetics, with a higher intensity level within the chemically treated samples “Chi”, as well as within the contaminated untreated control samples “Ctr”, if compared to the other features. Thus, Heatmap visualisation of “Chi” xenometabolome data matrix shows a persistence of the chemical xenometabolites. To investigate the data further, PCA is used to analyse “Chi” xenometabolome data matrix after a Log<sub>10</sub>-transformation and a Pareto scaling were applied (Fig. 7). The samples are projected on the 2 most relevant principal components: PC1 and PC2. PC1 explaining 80.6% of the variations is discriminating the chemically treated samples “Chi” in red from the contaminated untreated control samples “Ctr” in green. PC2 explaining 6.6% of the variations discriminates the heterogeneous contamination within the untreated control samples “Ctr”. It is also discriminating the chemically treated samples 7 days after T3 (T3t07) from the samples 14 days and 21 days after T3 (T3t14 and T3t21, respectively).

To investigate and understand the discriminations on the PC2, the Biplot of the PCA is observed (Fig. S10). The Biplot mainly highlights 4 features: 2 on the top of the Biplot correlating with the contaminated control samples 7 days and 14 days after T3, and 2 on the bottom of

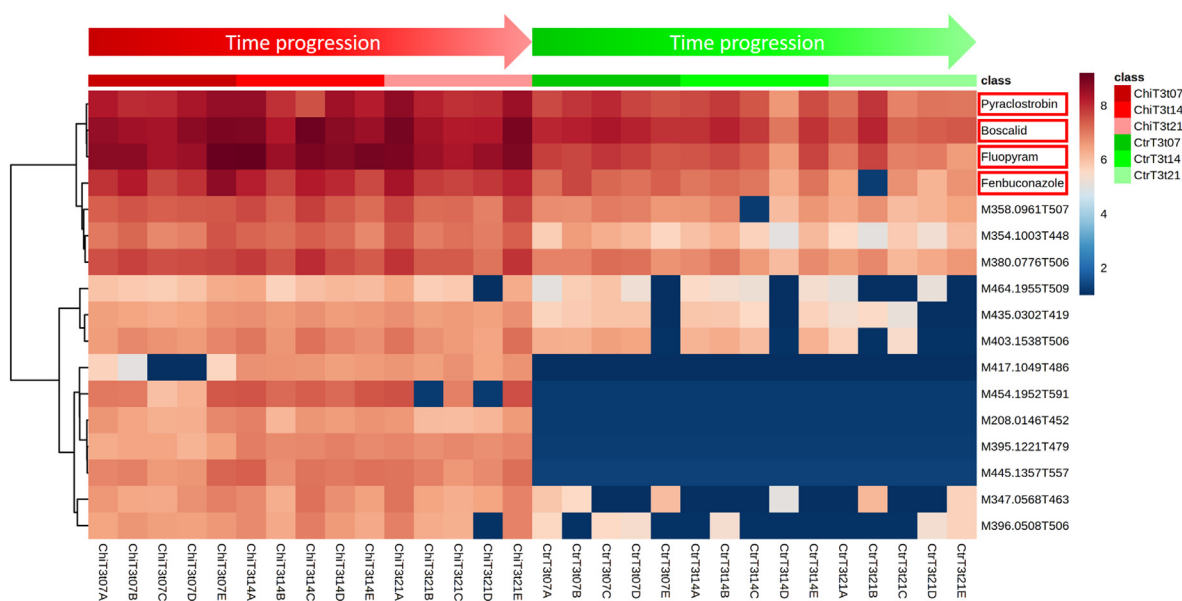


**Fig. 6.** Heatmap of Chemical reference xenometabolites abundance (the darker is the red, the higher is the intensity): “Chi” treated samples from 7 days (dark red) to 21 days (light red) after treatment, vs. “Ctr” untreated control samples from 7 days (dark green) to 21 days (light green) after treatment. Identified ASs’ molecular traces are circled in red.



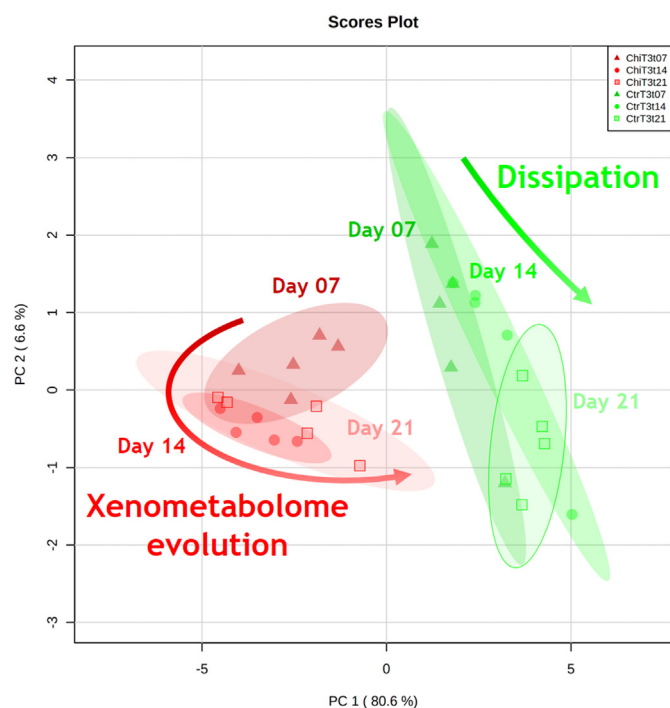


**Fig. 7.** PCA of the Chemical reference xenometabolites degradation kinetics: 7 days after the third treatment (T3) (T3t07), 14 days after T3 (T3t14), 21 days after T3 (T3t21) (from dark red to light red, respectively), and the contaminated untreated control (corresponding to T3t07, T3t14 and T3t21, from dark green to light green, respectively).

the biplot correlating with the contaminated control samples 21 days after T3 and also the chemically treated samples 14 days and 21 days after T3. Boxplots of these 4 features are shown in Fig. S10. Boxplots “A” and “B” of the features from the top of the biplot (Fig. S10) present, on one hand, high relative intensity levels within the treated samples “Chi” that persist through the time. However, within the contaminated untreated control samples “Ctr”, they generally show lower intensity levels when compared to the “Chi” treated samples at all the time points. Moreover, a dissipation pattern is observed through the time in those control samples, with a nearly complete dissipation 21 days after T3. On the other hand, boxplots “C” and “D” of the features from the bottom of the biplot (Fig. S10) show significantly low levels of contamination in the untreated control samples “Ctr” (nearly at the limit of the background noise or with intensities equal to 0). Concerning the chemically treated samples “Chi”, boxplots show a persistence along all the kinetics tracking for the feature “M347.0568T463” (D) (Fig. S10). For the other feature “M417.1049 T486” (C), boxplots (Fig. S10) show an appearance kinetics from 7 days to 14 days after T3 and a persistence from 14 days to 21 days after T3. These results showed that PCA is a tool that permit monitoring features through the kinetics. PCA is able to reveal a dissipation tendency of the contaminant xenometabolite features within the untreated control samples from 7 days after T3 to 21 days after T3. Moreover, PCA is able to discriminate the chemically treated samples 7 days after T3 from the 14 days and 21 days after T3, which can be explained by the appearance of some by-product patterns 14 days after T3 and persisting at the day 21 after T3 (with a slight tendency to head to the contaminated untreated control samples). These results are concordant with the OPLS-DA comparing the chemically treated samples vs. the contaminated untreated control samples after a  $\log_{10}$ -transformation and a Pareto scaling were applied on the datasets (Table S3). The OPLS-DA is validated for every time sampling ( $R^2_Y > R^2_X$ ,  $R^2_Y > Q^2$ ,  $R^2_Y - Q^2 \leq 30\%$ , and  $Q^2 > 50\%$  (Wiklund, 2008)). The values increase from 7 days ( $R^2_Y$ : 88.20%,  $Q^2$ : 85.10%) to 14 days after T3 ( $R^2_Y$ : 91.00%,  $Q^2$ : 89.90%) and

slightly decreases from 14 days to 21 days after T3 ( $R^2_Y$ : 91.00%,  $Q^2$ : 87.70%).

In order to quantify the 5 ASs (Boscalid, Pyraclostrobin, Fenbuconazole, Fluopyram and Tebuconazole) within the samples (“Ctr” and “Chi”) 21 days after the last Chemical reference treatment, standard addition method was applied. Calibration curves were drawn for each of the 5 chlorinated ASs integrating the areas of the “[M+H]<sup>+</sup><sub>-35</sub>Cl” ion and comparing them with those of the “[M+H]<sup>+</sup><sub>-37</sub>Cl” ion. The results were consistent for the 2 types of ions and all calibration curves had a calculated  $R^2 > 0.99$  (Fig. S11). The results are summarised in Table 2. 21 days after the last treatment, all the 5 compounds could be quantified. The values were obtained per gram of peach peel and converted to per gram of peach (fresh mass) (Formula S1). This “conversion” was done in order to compare the results with the thresholds considered by the E.U. regulation authorities as limit of quantification, and No Residue threshold (European Parliament and Council Of The European Union, 2005). This limit is defined as 10 ng/g of fresh mass. Most of the measured concentrations were upper than this threshold within the “Chi” samples (Table 2). Thus, 21 days after their application, ASs show persistence as they could be quantified within all the samples. 3 of the ASs (i.e. Pyraclostrobin, Boscalid, and Fluopyram) showed a high persistence within the peach peels of the treated samples, with concentrations between 2-times and 10-times higher than the No Residue threshold of 10 ng/g of fresh mass. The results obtained for the quantification are in agreement with the observations made previously with the statistical analyses: the 4 ASs (Boscalid, Pyraclostrobin, Fenbuconazole and Fluopyram) are more concentrated within the “Chi” samples than in the “Ctr” samples. Within “Ctr” samples, most of the ASs are lower than the No Residue threshold, except Boscalid that is higher with 23.68 ng/g of fresh mass. For Tebuconazole, the same concentrations were more or less obtained for control and treated samples (taking into account the SD). Its peach fresh mass concentration is lower than the No Residue threshold settled by regulation authorities (10 ng/g of fresh mass): 0.52 ng/g for “Ctr” samples and 0.18 ng/g for treated “Chi” samples. However, it should be mentioned that an important field samples variability could be underlined by the relatively high SD values (Table 2).

#### 4. Discussion

According to the results described above, EMF approach applied to peach peel matrix seems to be suitable to study the fate of botanical extracts like Akivi. In fact, Akivi’s xenometabolites were detected, separated from the peach endometabolites, and then tracked through time without the need for their identification at this stage of the study. Akivi’s xenometabolites evolution showed a clear dissipation kinetics along the samplings time points. Moreover, the statistical analyses allowed the observation of different xenometabolites patterns: features from the original Akivi BP more or less persistent, and degradation by-products. Hence, the EMF seems to be a reliable approach to study the fate of complex BPs with a partially or completely unknown biochemical composition. It also allows for the post-analysis filtration of the xenometabolome from the entire complex meta-metabolome, in order to provide a clear fate tracking by using different statistical approaches.

In the case of Armicarb® BP mineral extract, the analytical method used in this study (particularly, the use of the C18 Reverse-Phase LC (RPLC) column) is not adequate to detect its mineral AS ( $\text{KHCO}_3$ ) due to its high solubility in water. Probably, the potential development of some relatively adapted analytical methods in the future (e.g. those based on Ion Chromatography) may allow such an untargeted approach to study the fate of such compound families. Nonetheless, despite being unable to detect the AS *per se*, the EMF was able to discriminate between the treated and the untreated samples by detecting certain of Armicarb®’s xenometabolites. Most probably, those xenometabolites are the co-formulants and adjuvants of the formulated product that represent 15% (m/m) of its composition. They were

**Table 2**

Concentration of Chemical reference active substances measured within the untreated control samples "Ctr" and the Chemical reference treated samples "Chi" 21 days after the last treatment (means between 3 biological replicates).

Compound	Residues "Ctr" (ng/g) <sup>a</sup>	SD (ng/g) <sup>a</sup>	Residues "Chi" (ng/g) <sup>a</sup>	SD (ng/g) <sup>a</sup>	Residues "Ctr" (ng/g) <sup>b</sup>	Residues "Chi" (ng/g) <sup>b</sup>
<i>Pyraclostrobin</i>	138.25	90.51	681.48	185.04	4.60	22.69
<i>Boscalid</i>	711.23	470.29	3072.83	1550.44	23.68	102.33
<i>Fenbuconazole</i>	29.63	20.53	266.67	153.96	0.98	8.88
<i>Fluopyram</i>	118.52	59.29	1481.48	1068.33	3.95	49.33
<i>Tebuconazole</i>	15.76	9.06	5.27	0.74	0.52	0.18

The concentrations are expressed in ng/g of dried peach peel and in ng/g of peach fresh mass. Means above 10 ng/g of fresh mass are coloured in orange.

a: ng/g of dried peach peel; b: ng/g of peach fresh mass.

persistent all over the 14 days of the kinetics study. Therefore, the ability of the EMF to assess the fate of PPP formulation compounds in the crop or in the environment represents an important plus-value that might allow identifying a treated/polluted group of samples *via* the detection of PPPs' formulation ingredients, especially that those compounds usually represent a significant percentage of the total composition of the formulated product.

Concerning the Chemical reference treatment, the EMF approach was able to detect the 4 molecules pertaining to the ASs' of the 3 Chemical reference PPPs and some by-products features. It was thus able to discriminate between the treated and the untreated samples, despite the contamination of the untreated control samples by the applied PPPs (this contamination was identified because chlorinated compounds are not reported in peach endometabolome so far). The discrimination was feasible thanks to comparative semi-quantitative analysis of the EMF that takes in consideration the difference of PPP's components quantities between the two compared samples (treated vs. untreated). In the current case, the abundances of the PPP's AS were significantly higher in the treated samples. Furthermore, results analysis was able to reveal a potential dose-effect on the degradation kinetics. In fact, for the treated samples, where the quantity of the AS is significantly higher, a persistence pattern through time was observed for AS's compounds. On the other hand, in the contaminated control samples, where the quantity of the AS's compounds is relatively low, degradation patterns through time could be observed. Nevertheless, the contamination of control samples by the PPPs is still a significant issue for the EMF-based studies. In fact, the untreated control samples are taken as a basis to select the xenometabolome. In addition, the untreated control samples represent the "No Residues" point that must be reached in order to determine the "dissipation interval".

From all the described results, we can note that at the pre-harvest interval (PHI) of the 3 products that is set to 3 days, the residues dissipation is not reached neither for AS and co-formulants nor for by-products. However, it is worth to mention that the analyses were conducted using a high-resolution mass spectrometer that is able to detect molecular features with relatively high selectivity and sensitivity. This system allowed detecting the persistence of xenometabolites features at the last sampling point. These xenometabolites are detected with high signal-to-noise (S/N) over the limit of quantification (LOQ: S/N > 10), so the concentration of the features could be considered measurable. For instance, the 4 chlorinated compounds of the 3 Chemical reference products are still detected 21 days after the last treatment with a S/N > 10,000, *i.e.* significantly higher than the LOQ. These compounds were all quantified and three of them (*Pyraclostrobin*, *Boscalid*, *Fluopyram*) presented concentrations above the No Residue threshold settled by regulation authorities (10 ng/g of fresh mass) (European Parliament and Council Of The European Union, 2005). This quantification study confirms that at  $t = 21$  days after the last treatment, the xenometabolome was not dissipated. The quantification results are in

agreement with those obtained with our developed untargeted metabolomics approach. The methodology optimised in this work is highly sensitive and seems to be suitable to monitor the xenometabolome fate after the treatment of fruit matrix.

The novelty of this work is that it was conducted in the field, in contrast to the previous studies that were previously carried out in laboratory microcosms (Patil et al., 2016; Salvia et al., 2018). The current study was therefore confronted with some more difficulties that are important and must be taken into account. The first point, already mentioned, was the contamination of the untreated samples. This contamination issue could be hypothetically explained as the following: during the field experiments, the BPs and the Chemical reference were manually sprayed on the peach trees. Even if it was cautiously conducted, the spraying was directed to the top of the tree and some spray drift cannot be totally avoided. The cautious sampling method (Fig. S2) was not sufficient to prevent the fruits from being contaminated. For further studies, a better protection of the untreated control trees must be discussed, as isolating some untreated control trees on a corner of the orchard to decrease spray drift risks and take fruits from those control trees for residue monitoring. Spray drift may have occurred for all the studied treatments. For the chemical reference, the contamination of the samples (and in particular the untreated control samples "Ctr") was underlined thanks to the known chlorinated Chemical reference AS and the MS isotopic patterns of the chlorinated compounds (as no chlorinated compound are produced by the peach itself). However, a contamination by the Akivi cannot be verified as it is a natural extract and it is difficult to discriminate between its metabolites and the metabolites produced by the peach itself. Thus, this study was able to highlight that the spray drift is still an important phenomenon that can occur in field condition and must be taken into account in the future studies, especially as it can cause a serious problem for the untargeted metabolomics-based EMF approach.

Besides, working with biological samples always induces variability due to the multi-factor differences between plants, trees, leaves or fruits. In field conditions, the variability increases significantly because the soil is slightly different within the plot. Moreover, the trees receive a heterogeneous quantity of light, rain and wind compared to experiments in controlled conditions. In addition, focusing on this study, the fruits received a heterogeneous quantity of treatment because leaves around the fruit may hide part of the fruit and only the parts of the fruit exposed to the outside of the tree were treated. To reduce variability during the sampling, every sample is composed of the peel of 3 peaches and 5 repetitions are made for each time sampling. However, when studying the xenometabolome, an important variability appeared among the repetitions, which may mask some information. It appeared in particular on the Heatmaps (Figs. 2, 4, and 6) where some features had already disappeared in some repetition on a sampling time point and the same features were detected in the next sampling time point. It can be explained by the heterogeneous exposure of the fruits to the

treatment but also to light, wind, and rain that could cause a differential dissipation of the compounds between the repetitions of samples. For future field experiment, it would be interesting to collect more samples repetitions and include more fruits in the repetitions in order to limit variability between the biological repetitions.

All these points are highly important and it is interesting to consider them. They must be in-depth investigated in order to improve the field experimentations.

## 5. Conclusion

The current study aimed to adapt the EMF approach to fruit matrices and to target the xenometabolome in order to investigate the fate of BPs and the dissipation of their residues within treated crops. The EMF allowed to isolate post-analytically the xenometabolome from the total complex meta-metabolome and proved its ability to monitor the concentration evolution of the different components of the formulated PPPs (BPs and chemical PPP as well) within the studied matrix over the time. To conclude, no complete residues dissipation was reached for all the 3 studied treatments during the experiments that were carried out. The approach was proven reliable. Nonetheless, the experimental design should be improved for the future studies in order to avoid the contamination of the untreated control samples by spray drift during field treatment. Moreover, the sampling strategy should be improved in order to bypass the field-linked physical and biochemical variations.

## CRedit authorship contribution statement

**Mélina Ramos:** Conceptualisation, Investigation, Data processing, Visualisation, Writing – Original draft, **Hikmat Ghosson:** Investigation, Data processing, Visualisation, Writing – Original draft, **Delphine Raviglione:** Resources, **Cédric Bertrand:** Conceptualisation, Writing – Reviewing and Editing, **Marie-Virginie Salvia:** Conceptualisation, Writing – Reviewing and Editing.

## Declaration of competing interest

The authors declare that they have no known competing financial interests or personal relationships that could have appeared to influence the work reported in this paper.

## Acknowledgements

We are grateful towards Aude Lusetti from the Sica CENTREX who helped us for peach samplings and storage of the samples. We are thankful towards Vanessa Andreu from S.A.S. AkiNaO who helped us on the early stage of analysis optimisation with her expertise on Akivi BP chemical characteristics. The LC-Q/Orbitrap method development and analyses were performed using the Biodiversité et Biotechnologies Marines (Bio2Mar) facilities – Métabolites Secondaires Xénobiotiques Métabolomique Environnementale (MSXM) platform at the Université de Perpignan Via Domitia (<http://bio2mar.obs-banyuls.fr/>). This work was supported by PALVIP project that has been 65% co-financed by the European Regional Development Fund (ERDF) through the Interreg V-A Spain France Andorra programme (POCTEFA 2014-2022). POCTEFA aims to reinforce the economic and social integration of the French-Spanish-Andorran borders. Its support is focused on developing economic, social and environmental cross-border activities through joint strategies favouring sustainable territorial development.

## Appendix A. Supplementary data

Supplementary data to this article can be found online at <https://doi.org/10.1016/j.scitotenv.2021.150717>.

## References

- Chambers, M.C., Maclean, B., Burke, R., Amodei, D., Ruderman, D.L., Neumann, S., Gatto, L., Fischer, B., Pratt, B., Egerton, J., Hoff, K., Kessner, D., Tasman, N., Shulman, N., Frewen, B., Baker, T.A., Brusniak, M.-Y., Paulse, C., Creasy, D., Flashner, L., Kani, K., Moulding, C., Seymour, S.L., Nuwaysir, L.M., Lefebvre, B., Kuhlmann, F., Roark, J., Rainer, P., Detlev, S., Hemenway, T., Huhmer, A., Langridge, J., Connolly, B., Chadick, T., Holly, K., Eckels, J., Deutsch, E.W., Moritz, R.L., Katz, J.E., Agus, D.B., MacCoss, M., Tabb, D.L., Mallick, P., 2012. A cross-platform toolkit for mass spectrometry and proteomics. *Nat. Biotechnol.* 30, 918–920. <https://doi.org/10.1038/nbt.2377>.
- European Commission – Directorate General for Agriculture, 2000. *Guidance Document on Persistence in Soil (9188/VI/97 rev. 8)*.
- European Parliament, Council Of The European Union, 2005. *Regulation 396/2005/EC: On Maximum Residue Levels of Pesticides in or on Food and Feed of Plant and Animal Origin and Amending Council Directive 91/414/EEC, Regulation 396/2005/EC*.
- European Parliament, Council Of The European Union, 2009. *Directive 2009/128/EC: Establishing a Framework for Community Action to Achieve the Sustainable Use of Pesticides, Directive 2009/128/EC*.
- FAO, 2006. *Guidelines on Efficacy Evaluation for the Registration of Plant Protection Products*.
- Giacomoni, F., Le Corguillé, G., Monsoor, M., Landi, M., Pericard, P., Pétéra, M., Duperier, C., Tremblay-Franco, M., Martin, J.-F., Jacob, D., Goulitquer, S., Thévenot, E.A., Caron, C., 2015. Workflow4Metabolomics: a collaborative research infrastructure for computational metabolomics. *Bioinformatics* 31, 1493–1495. <https://doi.org/10.1093/bioinformatics/btu813>.
- Guillon, Y., Tremblay-Franco, M., Le Corguillé, G., Martin, J.-F., Pétéra, M., Roger-Mele, P., Delabrière, A., Goulitquer, S., Monsoor, M., Duperier, C., Canlet, C., Servien, R., Tardivel, P., Caron, C., Giacomoni, F., Thévenot, E.A., 2017. Create, run, share, publish, and reference your LC-MS, FIA-MS, GC-MS, and NMR data analysis workflows with the Workflow4Metabolomics 3.0 Galaxy online infrastructure for metabolomics. *Int. J. Biochem. Cell Biol.* 93, 89–101. <https://doi.org/10.1016/j.ijbiocel.2017.07.002>.
- ITAB, ONEMA, 2013. *Guide Pédagogique "Procédures réglementaires applicables aux produits de bio-contrôle"*.
- Kuhl, C., Tautenhahn, R., Böttcher, C., Larson, T.R., Neumann, S., 2012. CAMERA: an integrated strategy for compound spectra extraction and annotation of LC/MS data sets. *Anal. Chem.* 84, 283–289. <https://doi.org/10.1021/ac202450g>.
- Ministère de l'Agriculture et de l'Alimentation, 2015. *Écophyto* [WWW document]. URL Ministère de l'Agriculture et de l'Alimentation (accessed 10.8.20) <https://agriculture.gouv.fr/ecophyto>.
- Monnerie, S., Petera, M., Lyan, B., Gaudreau, P., Comte, B., Pujos-Guillot, E., 2019. Analytical correlation filtration: a new tool to reduce analytical complexity of metabolomic datasets. *Metabolites* 9, 250. <https://doi.org/10.3390/metabo9110250>.
- OECD, 2007a. *OECD guidelines for the testing of chemicals, section 5: other test guidelines* [WWW document]. URL [https://www.oecd-ilibrary.org/environment/oecd-guidelines-for-the-testing-of-chemicals-section-5-other-test-guidelines\\_20745796](https://www.oecd-ilibrary.org/environment/oecd-guidelines-for-the-testing-of-chemicals-section-5-other-test-guidelines_20745796) (accessed 9.3.21).
- OECD, 2007b. *Test No. 501: Metabolism in Crops (Guideline No. 501)*, OECD Guidelines for the Testing of Chemicals, Section 5. OECD, Paris.
- Pang, Z., Chong, J., Zhou, G., de Lima Morais, D.A., Chang, L., Barrette, M., Gauthier, C., Jacques, P.-É., Li, S., Xia, J., 2021. *MetaboAnalyst 5.0: narrowing the gap between raw spectra and functional insights*. *Nucleic Acids Res.* <https://doi.org/10.1093/nar/gkab382>.
- Patil, C., Calvayrac, C., Zhou, Y., Romdhane, S., Salvia, M.-V., Cooper, J.-F., Dayan, F.E., Bertrand, C., 2016. Environmental Metabolic Footprinting: a novel application to study the impact of a natural and a synthetic  $\beta$ -triketone herbicide in soil. *Sci. Total Environ.* 566–567, 552–558. <https://doi.org/10.1016/j.scitotenv.2016.05.071>.
- Rajski, Ł., Gómez-Ramos, M.del M., Fernández-Alba, A.R., 2014. Large pesticide multiresidue screening method by liquid chromatography-Orbitrap mass spectrometry in full scan mode applied to fruit and vegetables. *J. Chromatogr. A* 1360, 119–127. <https://doi.org/10.1016/j.chroma.2014.07.061>.
- Ramos, M., 2021. Development of an untargeted metabolomics approach for the impact evaluation of biocontrol product on plant holobiont and residues dissipation - W4M workflow and parameters [WWW document]. URL <https://workflow4metabolomics.usgalaxy.fr/u/mramos/w/peach-peel-2018-optimised-workflow> (accessed 2.25.21).
- Rizzetti, T.M., Kemmerich, M., Martins, M.L., Prestes, O.D., Adaime, M.B., Zanella, R., 2016. Optimization of a QuEChERS based method by means of central composite design for pesticide multiresidue determination in orange juice by UHPLC-MS/MS. *Food Chem.* 196, 25–33. <https://doi.org/10.1016/j.foodchem.2015.09.010>.
- Rutkowska, E., Łozowicka, B., Kaczyński, P., 2018. Modification of multiresidue QuEChERS protocol to minimize matrix effect and improve recoveries for determination of pesticide residues in dried herbs followed by GC-MS/MS. *Food Anal. Methods* 11, 709–724. <https://doi.org/10.1007/s12161-017-1047-3>.
- Salvia, M.-V., Ben Jrad, A., Raviglione, D., Zhou, Y., Bertrand, C., 2018. Environmental Metabolic Footprinting (EMF) vs. half-life: a new and integrative proxy for the discrimination between control and pesticides exposed sediments in order to further characterise pesticides' environmental impact. *Environ. Sci. Pollut. Res.* 25, 29841–29847. <https://doi.org/10.1007/s11356-017-9600-6>.
- Smith, C.A., Want, E.J., O'Maille, G., Abagyan, R., Siuzdak, G., 2006. XCMS: processing mass spectrometry data for metabolite profiling using nonlinear peak alignment, matching, and identification. *Anal. Chem.* 78, 779–787. <https://doi.org/10.1021/ac051437y>.
- Tamm, L., Schaerer, H.J., Levert, A., Andreu, V., Bertrand, C., 2017. *Agent antifongique, procédé et composition*. FR 3046907.
- Tautenhahn, R., Böttcher, C., Neumann, S., 2008. Highly sensitive feature detection for high resolution LC/MS. *BMC Bioinformatics* 9, 504. <https://doi.org/10.1186/1471-2105-9-504>.

Thévenot, E.A., Roux, A., Xu, Y., Ezan, E., Junot, C., 2015. Analysis of the human adult urinary metabolome variations with age, body mass index, and gender by implementing a comprehensive workflow for univariate and OPLS statistical analyses. *J. Proteome Res.* 14, 3322–3335. <https://doi.org/10.1021/acs.jproteome.5b00354>.

Trygg, J., Wold, S., 2002. Orthogonal projections to latent structures (O-PLS). *J. Chemometrics* 16, 119–128. <https://doi.org/10.1002/cem.695>.

van der Kloet, F.M., Bobeldijk, I., Verheij, E.R., Jellema, R.H., 2009. Analytical error reduction using single point calibration for accurate and precise metabolomic phenotyping. *J. Proteome Res.* 8, 5132–5141. <https://doi.org/10.1021/pr900499r>.

Wiklund, S., 2008. *Multivariate Data Analysis for Omics*.